Waves Propagation at an Interface of Two Liquid Saturated Porous Solid Half Spaces

Anup Singh [a], Vinod Kaliraman [b], Rajesh Kumar[c], Vipin Gupta[d] and M.S.Barak [e]

[a,b,c,d,e] *Department of Mathematics, Indira Gandhi University, Meerpur (Rewari), Haryana (India)*

Article History: Received: 10 January 2021; Revised: 12 February 2021; Accepted: 27 March 2021; Published online: 20 April 2021

Abstract: *This manuscript is concerned with reflected and refracted elastic waves when transverse waves are incident at the interface between two fluid-saturated porous solid half-spaces. Perfect and imperfect both types of contact of the interfaces are discussed. It has observed that for a specific model the behaviour of different reflected, refracted waves and the ratio of their amplitudes depend on the physical properties of the medium, angle of emergence, the porosity of the fluid, the porosity of fluid drenched incompressible porous medium and stiffness of imperfect boundary. The computer numerically results for this model have been presented graphically by taking a particular case of empty porous solid.*

Key words: *Amplitude ratios, Transverse wave, Elastic waves, porous liquid saturated solid, Reflection and Refraction*.

1. Introduction

The reflection and refraction characteristics of seismic waves are significant in predicting the underground deformations elastic and porous parameters. Bowen [1] applied the mixture theory principles on incompressible porous media models and developed a theory for determining the pore pressure of each pore fluid and stress equation for the mixture. Reflection and refraction of seismic waves incident obliquely at the boundary of a liquid-saturated porous solid has been discussed by Hajra and Mukhopadhayay [2]. In soil mechanics, Boer and Ethlers [3] historical reviewed the development and foundation of effective stress concept via mixture theory. In continuation, Boer et al. [4] analyzed the transient wave motion in fluid-saturated porous media and using Laplace transform technique derived the one-dimensional analytical solution. In a micropolar elastic layer, Kumar and Gogna [5] investigated the propagation of waves with stretch immersed in an infinite liquid and frequency equation for different types of vibrations.

One-dimensional transient wave propagation in fluid-saturated incompressible porous media has been studied by Kumar and Hundal [6] with the relation of discontinuities across the wavefronts and characteristic equation. An interface linking a micropolar liquid-saturated porous solid and homogenous inviscid liquid half-spaces refraction and reflection of seismic waves by Kumar and Barak [7]. Based on the theory of invariants, for a hyperelastic transversely isotropic solid, Ogden and Singh [8] derived the general constitutive equation. In a poroelastic solid saturated with three-phase viscous fluid, Santos and Gabriela [9] parametrically analyzed the waves propagation. Barak and Kaliraman [10], investigated the behaviour of elastic waves propagation at the interface of fluid-saturated incompressible porous solid and micropolar viscoelastic solid with different boundary conditions.

Recently, Reflection and Transmission of the plane wave at the surface and boundary of an elastic solid of dual permeability double-porosity materials have been obtained by Kumar et al. [11], [12]. At an imperfect interface, Barak and Kaliraman [13] studied the reflection and refraction of plane waves separating fluid saturated porous solid and micropolar elastic solid half-spaces. Barak et al. [14] analyzed the propagation of waves in partially saturated inhomogeneous soils. Kumar et al. [15] investigated the seismic waves reflection and refraction at the interface of a partially saturated soils and elastic solid in context of model developed by the Ghasemzadeh and Abounouri [16]. Keeping the above research in mind, in this manuscript we confine our attention towards characteristics of amplitude ratios of elastic waves at the perfect and imperfect interface of contact between two dissimilar porous solid half-spaces saturated with liquid, in which at the interface transverse waves are incident and amplitude ratios for a mixture of reflected and transmitted waves are computed numerically and depicted graphically for a specific model to understand the behavior of amplitude ratios that depends upon the angle of emergence, material properties of the medium, porosity of fluid drenched incompressible porous medium and stiffness of imperfect boundary.

Constructing the problem

Construct the problem in two-dimensional in which the interface z=0 separates fluid-saturated porous solid media $M_2[z<0]$ and $M_1[z>0]$ as shown in figure 2.1. The longitudinal or transverse wave propagates through the medium M_1 and incidents at the plane z=0 at an angle θ_0 with normal to the surface. The angle θ_1 and θ_2 be made by the two

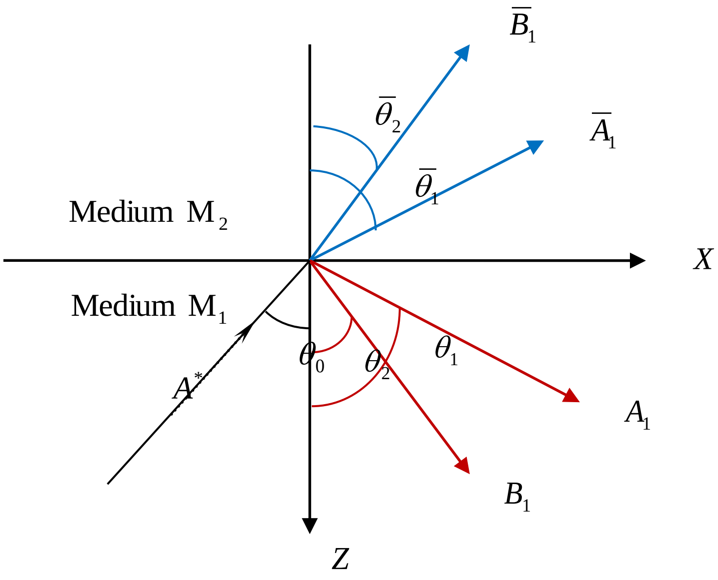

Geometry of the Problem

reflected waves P-wave and S-wave, respectively, with a positive direction of the z-axis in the medium M_1. Also, $\bar{\theta}_1$ and $\bar{\theta}_2$ be the angle made by the two transmitted waves P-wave and SV-wave respectively with the negative direction of z-axis in the medium M_2 , as shown in figure 2.1. A_1, B_1, $\bar{A}_1$ and $\bar{B}_1$ indicated the amplitude ratios of reflected and refracted waves in the medium M_1 and medium M_2, respectively.

3.1 **Basic Equations and Constitutive Relations for Medium** M_1

Governing equations for deformed incompressible porous medium drenched in the company of non-viscous fluid in the non-existence of body forces as discussed by [3] as follows

$$\nabla.\left(\eta^s \dot{u}_s + \eta^F \dot{u}_F\right) = 0 \tag{3.1.1}$$

$$\left(\lambda^S + \mu^S\right)\nabla(\nabla.u_S) + \mu^S\nabla^2 - \eta^S\nabla p - \rho^S\ddot{u}_S + S_v\left(\dot{u}_F - \dot{u}_S\right) = 0 \tag{3.1.2}$$

$$\eta^F\nabla p + \rho^F\ddot{u}_F + S_v\left(\dot{u}_F - \dot{u}_S\right) = 0 \tag{3.1.3}$$

$$T_E^S = 2\mu^S E_S + \lambda^S (E_S.I)I \tag{3.1.4}$$

$$E_S = \frac{1}{2}\left(grad\, u_S + grad^T u_S\right) \tag{3.1.5}$$

where, u_i represents the displacement, $\dot{u}_i$ velocity, $\ddot{u}_i$ acceleration, ρ density; ($i = F, S$) F for fluid and S for solid parts respectively and for incompressible pore fluid p denote effective pore pressure. Also, T_E^S represents stress and E_S the Langrangian strain tensor in the solid segment. λ^S and μ^S indicate the macroscopic Lame's parameters of porous solid and η^S, η^F the volume fractions satisfying the relation respectively

$$\eta^S + \eta^F = 1 \tag{3.1.6}$$

The tensor S_V relating the coupled interaction flanked by solid and fluid, in case of isotropic permeability written as

$$S_V = \frac{\left(\eta^F\right)^2 \gamma^{FR}}{K^F} I \tag{3.1.7}$$

where γ^{FR} and K^F are fluid's specific weight, and Darcy's permeability coefficient respectively. The displacement vector u_i (i = F, S for fluid and solid respectively) in two-dimensional problems can be taken as

$$u_i = \left(u^i, 0, w^i\right) \quad \text{where} \quad i = F, S. \tag{3.1.8}$$

Using equation (3.1.8) in equations (3.1.1) to (3.1.3), the following equations become

$$\left(\lambda^S + \mu^S\right)\frac{\partial \theta^S}{\partial x} + \mu^S \nabla^2 u^S - \eta^S \frac{\partial p}{\partial x} - \rho^S \frac{\partial^2 u^S}{\partial t^2} + S_V\left[\frac{\partial u^F}{\partial t} - \frac{\partial u^S}{\partial t}\right] = 0 \tag{3.1.9}$$

$$\left(\lambda^S + \mu^S\right)\frac{\partial \theta^S}{\partial z} + \mu^S \nabla^2 w^S - \eta^S \frac{\partial p}{\partial z} - \rho^S \frac{\partial^2 w^S}{\partial t^2} + S_V\left[\frac{\partial w^F}{\partial t} - \frac{\partial w^S}{\partial t}\right] = 0 \tag{3.1.10}$$

$$\eta^F \frac{\partial p}{\partial x} + \rho^F \frac{\partial^2 u^F}{\partial t^2} + S_V\left[\frac{\partial u^F}{\partial t} - \frac{\partial u^S}{\partial t}\right] = 0 \tag{3.1.11}$$

$$\eta^F \frac{\partial p}{\partial z} + \rho^F \frac{\partial^2 w^F}{\partial t^2} + S_V\left[\frac{\partial w^F}{\partial t} - \frac{\partial w^S}{\partial t}\right] = 0 \tag{3.1.12}$$

$$\eta^S\left[\frac{\partial^2 u^S}{\partial x \partial t} + \frac{\partial^2 w^s}{\partial z \partial t}\right] + \eta^F\left[\frac{\partial^2 u^F}{\partial x \partial t} + \frac{\partial^2 w^F}{\partial z \partial t}\right] = 0 \tag{3.1.13}$$

Also, ${t_{zx}}^S$ and ${t_{zz}}^S$ are tangential and normal stresses in solid part respectively may be written as

$${t_{zz}}^S = \lambda^S\left(\frac{\partial u^S}{\partial x} + \frac{\partial w^S}{\partial z}\right) + 2\mu^S \frac{\partial w^S}{\partial z} \tag{3.1.14}$$

$${t_{zx}}^S = \mu^S\left(\frac{\partial u^S}{\partial z} + \frac{\partial w^S}{\partial x}\right) \tag{3.1.15}$$

where

$$\theta^S = \frac{\partial\left(u^S\right)}{\partial x} + \frac{\partial\left(w^S\right)}{\partial x} \tag{3.1.16}$$

and

$$\nabla^2 \equiv \frac{\partial^2}{\partial x^2} + \frac{\partial^2}{\partial z^2} \tag{3.1.17}$$

In fluid and solid phase, displacement components (*i.e.* u^j and w^j) are associated with dimensional potential (i.e. ϕ^j and ψ^j) as

$$u^j = \frac{\partial \phi^j}{\partial x} + \frac{\partial \psi^j}{\partial z} \; and \; w^j = \frac{\partial \phi^j}{\partial z} - \frac{\partial \psi^j}{\partial x}; \quad j = F, S \tag{3.1.18}$$

Using equation (3.1.18), equations (3.1.9) to (3.1.13) can be written as

$$\nabla^2 \phi^S - \frac{1}{C^2}\frac{\partial^2 \phi^S}{\partial t^2} - \frac{S_V}{\left(\lambda^S + 2\mu^S\right)\left(\eta^F\right)^2}\frac{\partial \phi^S}{\partial t} = 0 \tag{3.1.19}$$

$$\phi^F = -\frac{\eta^S}{\eta^F}\phi^S \tag{3.1.20}$$

$$\mu^S \nabla^2 \psi^S - \rho^S \frac{\partial^2 \psi^S}{\partial t^2} + S_V\left[\frac{\partial \psi^F}{\partial t} - \frac{\partial \psi^S}{\partial t}\right] = 0 \tag{3.1.21}$$

$$\rho^F \frac{\partial^2\psi^F}{\partial t^2} + S_V\left[\frac{\partial\psi^F}{\partial t} - \frac{\partial\psi^S}{\partial t} = 0\right] \tag{3.1.22}$$

$$\left(\eta^F\right)^2 p - \eta^S \rho^F \frac{\partial^2\phi^S}{\partial^2 t} - S_V \frac{\partial\phi^S}{\partial t} = 0 \tag{3.1.23}$$

where

$$C = \sqrt{\frac{\left(\eta^F\right)^2\left(\lambda^S + 2\mu^S\right)}{\left(\eta^F\right)^2\rho^S + \left(\eta^S\right)^2\rho^F}} \tag{3.1.24}$$

Consider the solutions (3.1.19) to (3.1.23) in the form

$$\left(\phi^S, \phi^F, \psi^S, \psi^F, p\right) = \left(\phi_1^S, \phi_1^F, \psi_1^S, \psi_1^F, p_1\right)\exp(i\omega t) \tag{3.1.25}$$

where ω represent complex circular frequency.
Using (3.1.25) in equations (3.1.19) to (3.1.23), we obtain

$$\left[\nabla^2 + \frac{\omega^2}{c_1^{\,2}} - \frac{i\omega S_V}{(\lambda^S + 2\mu^S)(\eta^F)^2}\right]\phi_1^{\,S} = 0 \tag{3.1.26}$$

$$\left[\mu^S\nabla^2 + \rho^S\omega^2 - i\omega S_V\right]\psi_1^{\,S} = -i\omega S_V \psi_1^{\,F} \tag{3.1.27}$$

$$\left[-\omega^2\rho^F + i\omega S_V\right]\psi_1^{\,F} - i\omega S_V\psi_1^{\,S} = 0 \tag{3.1.28}$$

$$(\eta^F)^2 p_1 + \eta^S\rho^F\omega^2\phi_1^{\,S} + i\omega S_V\phi_1^{\,S} = 0 \tag{3.1.29}$$

$$\phi_1^{\,F} = -\frac{\eta^S}{\eta^F}\phi_1^{\,S} \tag{3.1.30}$$

Equation (3.1.26) corresponds to a longitudinal wave propagating with velocity V_1, given by

$$V_1^{\,2} = \frac{1}{G_1} \tag{3.1.31}$$

where

$$G_1 = \left[\frac{1}{C_1^{\,2}} - \frac{iS_V}{\omega(\lambda^S + 2\mu^S)(\eta^F)^2}\right] \tag{3.1.32}$$

From equation (3.1.27) and (3.1.28), we obtain

$$\left[\nabla^2 + \frac{\omega^2}{V_2^{\,2}}\right]\psi_1^{\,S} = 0 \tag{3.1.33}$$

Equation (3.1.33) for the propagation of transverse wave with velocity V_2, given by

$$V_2^{\,2} = \frac{1}{G_2}$$

where

$$G_2 = \left\{\frac{\rho^s}{\mu^s} - \frac{iS_V}{\mu^S\omega} - \frac{S_V^{\,2}}{\mu^S\left(-\rho^S\omega^2 + i\omega S_V\right)}\right\} \tag{3.1.34}$$

3.2 **Constitutive Relations and Basic Equations for M_2**

The governing equations of the deformed medium M_2 in without body forces obtained by [3] as follows

$$\nabla.\left(\overline{\eta}^s\dot{\overline{u}}_s + \eta^F\dot{\overline{u}}_F\right) = 0 \tag{3.2.1}$$

$$\left(\overline{\lambda}^S + \overline{\mu}^S\right)\nabla\left(\nabla.\overline{u}_S\right) + \overline{\mu}^S\nabla^2 - \overline{\eta}^S\nabla\overline{p} - \overline{\rho}^S\ddot{\overline{u}}_S + S_v\left(\dot{\overline{u}}_F - \dot{\overline{u}}_S\right) = 0 \tag{3.2.2}$$

$$\bar{\eta}^F \nabla \bar{p} + \bar{\rho}^F \ddot{\bar{u}}_F + \bar{S}_v \left(\dot{\bar{u}}_F - \dot{\bar{u}}_S \right) = 0 \tag{3.2.3}$$

$$\bar{T}_E^S = 2\bar{\mu}^S \bar{E}_S + \bar{\lambda}^S (\bar{E}_S . I) I \tag{3.2.4}$$

$$\bar{E}_S = \frac{1}{2}\left(grad\, \bar{u}_S + grad^T \bar{u}_S \right) \tag{3.2.5}$$

$\bar{u}_i, \dot{\bar{u}}_i, \ddot{\bar{u}}_i ; i = F, S$ Symbolize displacement, velocities and acceleration of fluid and solid parts respectively, and for incompressible pore fluid $\bar{p}$ is effective pore pressure. $\bar{\rho}^S$ and $\bar{\rho}^F$ represent densities of solid and fluid. $\bar{T}_E^{\ S}$ Denote stress in solid part and $\bar{E}_S$ is linearized Langrangian strain tensor. $\bar{\lambda}^S$ and $\bar{\mu}^S$ are macroscopic Lame's parameters of porous solid and $\bar{\eta}^S$ and $\bar{\eta}^F$ are volume fractions fulfilling the relation.

$$\bar{\eta}^S + \bar{\eta}^F = 1 \tag{3.2.6}$$

In isotropic permeability case, tensors S_V relating coupled interaction between fluid and solid have been specified by

$$S_V = \frac{(\bar{\eta}^F)^2 \bar{\gamma}^{FR}}{\bar{K}^F} I \tag{3.2.7}$$

where $\bar{\gamma}^{FR}$ is fluid specific weight, $\bar{K}^F$ is the coefficient of Darcy's permeability. Assuming, displacement vector $\bar{u}_i \left(i = F, S \right)$ as

$$\bar{u}_i = \left(\bar{u}_i, 0, \bar{w}_i \right) \text{ where } i = F, S \tag{3.2.8}$$

Using equation (3.2.8) in equations (3.2.1) to (3.2.3), the following equations obtained as

$$\left(\bar{\lambda}^S + \bar{\mu}^S \right) \frac{\partial \bar{\theta}^S}{\partial x} + \bar{\mu}^S \nabla^2 \bar{u}^S - \bar{\eta}^S \frac{\partial \bar{p}}{\partial x} - \bar{\rho}^S \frac{\partial^2 \bar{u}^S}{\partial t^2} + \bar{S}_V \left[\frac{\partial \bar{u}^F}{\partial t} - \frac{\partial \bar{u}^S}{\partial t} \right] = 0 \tag{3.2.9}$$

$$\left(\bar{\lambda}^S + \bar{\mu}^S \right) \frac{\partial \bar{\theta}^S}{\partial z} + \bar{\mu}^S \nabla^2 \bar{w}^S - \bar{\eta}^S \frac{\partial \bar{p}}{\partial z} - \bar{\rho}^S \frac{\partial^2 \bar{w}^S}{\partial t^2} + \bar{S}_V \left[\frac{\partial \bar{w}^F}{\partial t} - \frac{\partial \bar{w}^S}{\partial t} \right] = 0 \tag{3.2.10}$$

$$\bar{\eta}^F \frac{\partial \bar{p}}{\partial x} + \bar{\rho}^F \frac{\partial^2 \bar{u}^F}{\partial t^2} + \bar{S}_V \left[\frac{\partial \bar{u}^F}{\partial t} - \frac{\partial \bar{u}^S}{\partial t} \right] = 0 \tag{3.2.11}$$

$$\bar{\eta}^F \frac{\partial \bar{p}}{\partial z} + \bar{\rho}^F \frac{\partial^2 \bar{w}^F}{\partial t^2} + \bar{S}_V \left[\frac{\partial \bar{w}^F}{\partial t} - \frac{\partial \bar{w}^S}{\partial t} \right] = 0 \tag{3.2.12}$$

$$\bar{\eta}^S \left[\frac{\partial^2 \bar{u}^S}{\partial x \partial t} + \frac{\partial^2 \bar{w}^s}{\partial z \partial t} \right] + \bar{\eta}^F \left[\frac{\partial^2 \bar{u}^F}{\partial x \partial t} + \frac{\partial^2 \bar{w}^F}{\partial z \partial t} \right] = 0 \tag{3.2.13}$$

Also, $\bar{t}_{zx}^{\ S}$ and $\bar{t}_{zz}^{\ S}$ are tangential and normal stresses in solid part respectively written as
In the fluid and solid phase,

$$\bar{t}_{zz}^{\ S} = \bar{\lambda}^S \left(\frac{\partial \bar{u}^S}{\partial x} + \frac{\partial \bar{w}^S}{\partial z} \right) + 2\bar{\mu}^S \frac{\partial \bar{w}^S}{\partial z} \tag{3.2.14}$$

$$\bar{t}_{zx}^{\ S} = \bar{\mu}^S \left(\frac{\partial \bar{u}^S}{\partial z} + \frac{\partial \bar{w}^S}{\partial x} \right) \tag{3.2.15}$$

where

$$\bar{\theta}^S = \frac{\partial \left(\bar{u}^S \right)}{\partial x} + \frac{\partial \left(\bar{w}^S \right)}{\partial x} \tag{3.2.16}$$

and

$$\nabla^2 \equiv \frac{\partial^2}{\partial x^2} + \frac{\partial^2}{\partial z^2} \tag{3.2.17}$$

displacement components (i.e. $\bar{u}^j$ and $\bar{w}^j$) are associated with dimensional potential (i.e. $\bar{\phi}^j$ and $\bar{\psi}^j$) as

$$\bar{u}^j = \frac{\partial \bar{\phi}^j}{\partial x} + \frac{\partial \bar{\psi}^j}{\partial z} \; and \; \bar{w}^j = \frac{\partial \bar{\phi}^j}{\partial z} - \frac{\partial \bar{\psi}^j}{\partial x}; \;\; j = F, S \tag{3.2.18}$$

Using equation (3.2.18), equations (3.2.9) to (3.2.13) becomes

$$\nabla^2 \bar{\phi}^S - \frac{1}{\bar{C}^2}\frac{\partial^2 \bar{\phi}^S}{\partial t^2} - \frac{\bar{S}_V}{\left(\bar{\lambda}^S + 2\bar{\mu}^S\right)\left(\bar{\eta}^F\right)^2}\frac{\partial \bar{\phi}^S}{\partial t} = 0 \tag{3.2.19}$$

$$\bar{\phi}^F = -\frac{\bar{\eta}^S}{\bar{\eta}^F}\bar{\phi}^S \tag{3.2.20}$$

$$\bar{\mu}^S \nabla^2 \bar{\psi}^S - \bar{\rho}^S \frac{\partial^2 \bar{\psi}^S}{\partial t^2} + \bar{S}_V\left[\frac{\partial \bar{\psi}^F}{\partial t} - \frac{\partial \bar{\psi}^S}{\partial t}\right] = 0 \tag{3.2.21}$$

$$\bar{\rho}^F \frac{\partial^2 \bar{\psi}^F}{\partial t^2} + \bar{S}_V\left[\frac{\partial \bar{\psi}^F}{\partial t} - \frac{\partial \bar{\psi}^S}{\partial t} = 0\right] \tag{3.2.22}$$

$$\left(\bar{\eta}^F\right)^2 \bar{p} - \bar{\eta}^S \bar{\rho}^F \frac{\partial^2 \bar{\phi}^S}{\partial^2 t} - \bar{S}_V \frac{\partial \bar{\phi}^S}{\partial t} = 0 \tag{3.2.23}$$

where

$$\bar{C} = \sqrt{\frac{(\bar{\eta}^F)^2(\bar{\lambda}^S + 2\bar{\mu}^S)}{(\bar{\eta}^F)^2\bar{\rho}^S + (\bar{\eta}^S)^2\bar{\rho}^F}} \tag{3.2.24}$$

Considering the solution of the system of equations (3.2.19) to (3.2.23) in the form

$$\left(\bar{\phi}^S, \bar{\phi}^F, \bar{\psi}^S, \bar{\psi}^F, \bar{p}\right) = \left(\bar{\phi}_1^S, \bar{\phi}_1^F, \bar{\psi}_1^S, \bar{\psi}_1^F, \bar{p}_1\right)\exp\left(i\bar{\omega}t\right) \tag{3.2.25}$$

where ω is the complex circular frequency. Making use of (3.2.25) in equations (3.2.19) to (3.2.23), we obtain

$$\left[\nabla^2 + \frac{\bar{\omega}^2}{\bar{c}_1^2} - \frac{i\omega\bar{S}_V}{(\bar{\lambda}^S + 2\bar{\mu}^S)(\bar{\eta}^F)^2}\right]\bar{\phi}_1^S = 0 \tag{3.2.26}$$

$$\left[\bar{\mu}^S\nabla^2 + \bar{\rho}^S\bar{\omega}^2 - i\bar{\omega}S_V\right]\psi_1^S = -i\omega S_V \psi_1^F \tag{3.2.27}$$

$$\left[-\bar{\omega}^2\bar{\rho}^F + i\bar{\omega}\bar{S}_V\right]\bar{\psi}_1^F - i\bar{\omega}\bar{S}_V\bar{\psi}_1^S = 0 \tag{3.2.28}$$

$$\left(\bar{\eta}^F\right)^2 \bar{p}_1 + \bar{\eta}^S\bar{\rho}^F\bar{\omega}^2\bar{\phi}_1^S + i\bar{\omega}\bar{S}_V\bar{\phi}_1^s = 0 \tag{3.2.29}$$

$$\bar{\phi}_1^F = -\frac{\bar{\eta}^S}{\bar{\eta}^F}\bar{\phi}_1^S \tag{3.2.30}$$

Equation (3.2.26) corresponds to a longitudinal wave propagating with velocity V_1, given by

$$\bar{V}_1^2 = \frac{1}{\bar{G}_1} \tag{3.2.31}$$

where

$$\bar{G}_1 = \left[\frac{1}{\bar{C}_1^2} - \frac{i\bar{S}_V}{\bar{\omega}(\bar{\lambda}^S + 2\bar{\mu}^S)(\bar{\eta}^F)^2}\right] \tag{3.2.32}$$

From equation (3.2.27) and (3.2.28), we obtain

$$\left[\nabla^2 + \frac{\overline{\omega}^2}{\overline{V}_2^{\,2}}\right]\overline{\psi}_1^{\,S} = 0 \tag{3.2.33}$$

Equation (3.1.33) corresponds to a transverse wave propagating with velocity V_2, given by

$$\overline{V}_2^{\,2} = \frac{1}{\overline{G}_2}, \text{ where } \quad \overline{G}_2 = \left\{\frac{\overline{\rho}^s}{\overline{\mu}^s} - \frac{i\overline{S}_V}{\overline{\mu}^S\overline{\omega}} - \frac{\overline{S}_V^{\,2}}{\overline{\mu}^S(-\overline{\rho}^S\overline{\omega}^2 + i\overline{\omega}\overline{S}_V)}\right\} \tag{3.2.34}$$

4.1 **The velocity Potentials and Pore Pressure for Medium** M_1

The potential function satisfying equations (3.1.19) to (3.1.23) written as

$$\phi^S = A_{01}\exp\{ik_1(x\sin\theta_0 - z\cos\theta_0) + i\omega_1 t\} + A_1\exp\{ik_1(x\sin\theta_1 + z\cos\theta_1) + i\omega_1 t\}$$
$$\phi^F = m_1 A_{01}\exp\{ik_1(x\sin\theta_0 - z\cos\theta_0) + i\omega_1 t\} + A_1\exp\{ik_1(x\sin\theta_1 + z\cos\theta_1) + i\omega_1 t\}$$
$$p = m_2 A_{01}\exp\{ik_1(x\sin\theta_0 - z\cos\theta_0) + i\omega_1 t\} + A_1\exp\{ik_1(x\sin\theta_1 + z\cos\theta_1) + i\omega_1 t\} \tag{4.1.1}$$
$$\psi^S = B_{01}\exp\{ik_2(x\sin\theta_0 - z\cos\theta_0) + i\omega_2 t\} + B_1\exp\{ik_2(x\sin\theta_2 + z\cos\theta_2) + i\omega_2 t\}$$
$$\psi^F = m_3 B_{01}\exp\{ik_2(x\sin\theta_0 - z\cos\theta_0) + i\omega_2 t\} + B_1\exp\{ik_2(x\sin\theta_2 + z\cos\theta_2) + i\omega_2 t\} \tag{4.1.2}$$

where

$$m_1 = -\frac{\eta^S}{\eta^F};\ m_2 = \left[\frac{\eta^S\omega_1^2\rho^F - i\omega_1 S_V}{(\eta^F)^2}\right] and\, m_3 = \frac{i\omega_2 S_V}{i\omega_2 S_V - \omega_2^{\,2}\rho^F} \tag{4.1.3}$$

and A_1, B_1 A_{01}, B_{01} are amplitudes of reflected P-wave and SV-wave, incident P-wave and SV-wave, respectively and their wave numbers of reflected waves are denoted by k_1 and k_2 respectively.

4.2 **The Velocity Potentials and Pore Pressure for Medium** M_2

The potential function satisfying equations (3.2.19) to (3.2.23) can be written as

$$\{\overline{\phi}^S, \overline{\phi}^F, \overline{p}\} = \{1, \overline{m}_1, \overline{m}_2\}\left[\overline{A}_1\exp\{i\overline{k}_1(x\sin\overline{\theta}_1 + z\cos\overline{\theta}_1) + i\overline{\omega}_1 t\}\right] \tag{4.2.1}$$
$$\{\overline{\psi}^S, \overline{\psi}^F\} = \{1, \overline{m}_3\}\left[\overline{B}_1\exp\{i\overline{k}_2(x\sin\overline{\theta}_2 + z\cos\overline{\theta}_2) + i\overline{\omega}_2 t\}\right] \tag{4.2.2}$$

where, $\overline{k}_1$, $\overline{A}_1$ are the wave number and amplitude of transmitted P wave and $\overline{k}_2$, $\overline{A}_2$ are the wave number and amplitude of transmitted SV- wave)

$$\overline{m}_1 = -\frac{\overline{\eta}^S}{\overline{\eta}^F};\ \overline{m}_2 = \left[\frac{\overline{\eta}^S\overline{\omega}_1^2\overline{\rho}^F - i\overline{\omega}_1\overline{S}_V}{(\overline{\eta}^F)^2}\right] and\, \overline{m}_3 = \frac{i\overline{\omega}_2\overline{S}_V}{i\overline{\omega}_2\overline{S}_V - \overline{\omega}_2^{\,2}\overline{\rho}^F} \tag{4.2.3}$$

5.1. **Case I: When the contact of the media is perfect**

At the interface z=0, the suitable boundary conditions in this case for the model under consideration are taken in mathematical form as

$$t_{zz}^S - p = \bar{t}_{zz}^S - \overline{p};\ t_{ZX}^s = \bar{t}_{ZX}^S;\ w^S = \overline{w}^s;\ u^S = \overline{u}^s \tag{5.1.1}$$

In order to gratify above said boundary conditions, the Snell's law extension written as

$$\frac{\sin\theta_0}{V_0} = \frac{\sin\theta_1}{V_1} = \frac{\sin\theta_2}{V_2} = \frac{\sin\overline{\theta}_1}{\overline{V}_1} = \frac{\sin\overline{\theta}_2}{\overline{V}_2} \tag{5.1.2}$$

Also, $k_1V_1 = k_2V_2 = \bar{k}_1\overline{V}_1 = \bar{k}_2\overline{V}_2 = \omega$ at $Z = 0$ (5.1.3)

where, $\overline{V}_1$ and $\overline{V}_2$ are velocities of the transmitted P and SV-wave respectively. For emergent P-wave

$$V_0 = V_1,\ \theta_0 = \theta_1 \tag{5.1.4}$$

For emergent SV-wave

$$V_0 = V_2,\ \theta_0 = \theta_2 \tag{5.1.5}$$

At boundary z=0, put $B_{01} = 0$ for incident P wave in equation (4.1.2) and $A_{01} = 0$ for incident SV-wave in equation (4.1.1). Using the potentials from (4.1.1 and 4.1.2) and (4.2.1 and 4.2.2) in relations (3.1.14, 15, 18) and

(3.2.14, 15, 18) respectively and using the relations (5.1.1 to 5), for obtaining four non-homogeneous equations system

$$\sum_{j=0}^{4} a_{ij} Z_j = Y_i \quad (i = 1,2,3,4) \tag{5.1.6}$$

where, $Z_1 = \frac{A_1}{A^*}$, $Z_2 = \frac{A_2}{A^*}$, $Z_3 = \frac{\bar{A}_1}{A^*}$, $Z_4 = \frac{\bar{B}_1}{A^*}$

The components a_{ij} and Y_i in equation (5.1.6) in the dimensionless form are as under

$$a_{11} = \frac{\lambda^S}{\mu^S} + 2\cos^2\theta_1 + \frac{m_2}{\mu^S k_1^2},\quad a_{12} = -2\sin\theta_2\cos\theta_2 \frac{k_2^2}{k_1^2},\quad a_{13} = \frac{-\bar{k}_1^2}{k_1^2\mu^S}\left[\bar{\lambda}^S + 2\bar{\mu}^S\cos^2\bar{\theta}_1 + \frac{\bar{m}_2}{\bar{k}_1^2}\right]$$

$$a_{14} = -\frac{\bar{\mu}^S \bar{k}_2^2}{\bar{k}_1^2 \mu^s}\sin 2\bar{\theta}_2,\quad a_{21} = 2\sin\theta_1\cos\theta_1,\quad a_{22} = \frac{k_2^2}{k_1^2}\left(\cos^2\theta_2 - \sin^2\theta_2\right),\quad a_{23} = \frac{\bar{\mu}^S \bar{k}_1^2}{k_1^2\mu^S} 2\sin\bar{\theta}_1,$$

$$a_{24} = -\frac{\bar{\mu}^S \bar{k}_2^2}{k_1^2\mu^S} 2\cos 2\bar{\theta}_2,\quad a_{31} = i\sin\theta_1,\quad a_{32} = \frac{ik_2\cos\theta_2}{k_1},\quad a_{33} = -\frac{i\bar{k}_1}{k_1}\sin\bar{\theta}_1,\quad a_{34} = \frac{i\bar{k}_2\cos\bar{\theta}_2}{k_1}$$

$$a_{41} = i\cos\theta_1,\quad a_{42} = -\frac{ik_2\sin\theta_2}{k_1},\quad a_{43} = \frac{i\bar{k}_1\cos\bar{\theta}_1}{k_1} \text{ and } a_{44} = \frac{i\bar{k}_2\sin\bar{\theta}_2}{k_1} \tag{5.1.8}$$

For incident P-wave; $A^* = A_{01}$, $Y_1 = -a_{11}$, $Y_2 = a_{21}$, $Y_3 = -a_{31}$ and $Y_4 = a_{41}$ (5.1.9)

For incident SV-wave; $A^* = B_{01}$, $Y_1 = a_{12}$, $Y_2 = -a_{22}$, $Y_3 = a_{32}$ and $Y_4 = -a_{42}$ (5.1.10)

Special Case: Either gas is filled in pores or there is no pores of medium M_1, and M_2 then both the mediums reduce to empty porous solids. In this case ρ^F and $\bar{\rho}^F$ are very small in comparison to ρ^S and $\bar{\rho}^S$ respectively and so, these can be neglected. So the relations (3.1.24) and (3.2.24) give us

$$C_0 = \sqrt{\frac{\lambda^S + 2\mu^S}{\rho^S}};\qquad \bar{C}_0 = \sqrt{\frac{\bar{\lambda}^S + 2\bar{\mu}^S}{\bar{\rho}^S}} \tag{5.1.11}$$

and the coefficients a_{11} and a_{13} in (5.1.8) changes to

$$a_{11} = \frac{\lambda^S}{\mu^S} + 2\cos^2\theta_1,\quad a_{13} = \frac{-\bar{k}_1^2}{k_1^2\mu^S}\left[\bar{\lambda}^S + 2\bar{\mu}^S\cos^2\bar{\theta}_1\right]$$

whereas, all the rest coefficients in (5.1.8) are the same.

5.2. **Case II: When the contact of the media is imperfect**

The values of boundary parameters depend on microstructure and also on bi-material properties of medium under consideration. The interface z=0 separated the two liquid with different density within the liquid saturated porous solid, the possible boundary conditions for such type of model are taken in the mathematical form as follows;

$$t_{ZZ}^S - p = \bar{t}_{ZZ}^S - \bar{p},\quad t_{ZX}^S = \bar{t}_{ZX}^S,\quad \bar{t}_{ZZ}^S - \bar{p} = k_n\left(u^S - \bar{u}^S\right) \text{ and } \bar{t}_{ZX}^S = k_t\left(u^S - \bar{u}^S\right) \tag{5.2.1}$$

At the interface z=0, put $B_{01} = 0$ for incident P wave in equation (3.1.33) and $A_{01} = 0$ for incident SV-wave in equation (4.1.1), and using the potential functions from (4.2.1,2), (3.1.14,15,18) and (3.2.14,15,18) respectively and using the equations (6.2) and (5.1.2-5), for obtaining four non-homogeneous equations system

$$\sum_{j=0}^{4} a_{ij} Z_j = Y_i \quad (i = 1,2,3,4) \tag{5.2.2}$$

where $Z_1 = \frac{A_1}{A^*}$, $Z_2 = \frac{A_2}{A^*}$, $Z_3 = \frac{\bar{A}_1}{A^*}$ and $Z_4 = \frac{\bar{B}_1}{A^*}$ (5.2.3)

The components a_{ij} and Y_i in equation (5.2.2) in the dimensionless form are the same component as in (5.1.8) only the following component are different,

$$a_{33} = -\frac{i\bar{k}_1}{k_1}\sin\bar{\theta}_1 - \frac{\bar{\mu}^S \bar{k}_1^{\,2}\sin 2\bar{\theta}_1}{k_t k_1},\quad a_{34} = \frac{i\bar{k}_2\cos\bar{\theta}_2}{k_1} + \frac{\bar{\mu}^S \bar{k}_2^{\,2}\cos 2\bar{\theta}_2}{k_t k_1},$$

$$a_{43} = \frac{i\bar{k}_1\cos\bar{\theta}_1}{k_1} + \frac{\bar{k}_1^{\,2}\left[\bar{\lambda}^S + 2\bar{\mu}^S\cos^2\bar{\theta}_1 + \frac{\bar{m}_2}{\bar{k}_1^{\,2}}\right]}{k_n k_1},\quad a_{44} = \frac{i\bar{k}_2\sin\bar{\theta}_2}{k_1} + \frac{\bar{\mu}^S \bar{k}_2^{\,2}\sin 2\bar{\theta}_2}{k_n k_1} \qquad (5.2.4)$$

For incident P-wave; $A^* = A_{01}$, $Y_1 = -a_{11}$, $Y_2 = a_{21}$, $Y_3 = -a_{31}$ and $Y_4 = a_{41}$ (5.2.5)

For incident SV-wave; $A^* = B_{01}$, $Y_1 = a_{12}$, $Y_2 = -a_{22}$, $Y_3 = a_{32}$ and $Y_4 = -a_{42}$ (5.2.6)

5.3. **Particular Cases**

Case I: $(k_n \neq 0, k_t \to \infty)$ Normal force stiffness

A system of four non homogeneous equations is obtained in this case, as in equation (5.2.2), where all a_{ij} are same except values of a_{33} and a_{34} are as

$$a_{33} = -\frac{i\bar{k}_1}{k_1}\sin\bar{\theta}_1,\quad a_{34} = \frac{i\bar{k}_2\cos\bar{\theta}_2}{k_1} \qquad (5.2.7)$$

Case II: $(k_t \neq 0, k_n \to \infty)$ Transverse force stiffness

A system of four non homogeneous equations is obtained in this case, as in equation (5.2.2), where all a_{ij} are same except values of a_{43} and a_{44} are as

$$a_{43} = \frac{i\bar{k}_1\cos\bar{\theta}_1}{k_1},\quad a_{44} = \frac{i\bar{k}_2\sin\bar{\theta}_2}{k_1} \qquad (5.2.8)$$

Case III: when contact is welded $(k_n \to \infty, k_t \to \infty)$

Again for obtaining four non-homogeneous equations system (5.2.2), where all a_{ij} are same except values of $a_{33}, a_{34}, a_{43}\, and\, a_{44}$ are as

$$a_{33} = -\frac{i\bar{k}_1}{k_1}\sin\bar{\theta},\quad a_{34} = \frac{i\bar{k}_2\cos\bar{\theta}_2}{k_1},\quad a_{43} = \frac{i\bar{k}_1\cos\bar{\theta}_1}{k_1},\quad a_{44} = \frac{i\bar{k}_2\sin\bar{\theta}_2}{k_1} \qquad (5.2.9)$$

6 Numerical Results and Discussion

In order to understand the behavior of different amplitude ratios, in detail, these ratios are computed numerically for this model by considering the values of applicable different elastic parameters for medium M_1 are given [3] as

$$\eta^S = 0.67,\ \eta^F = 0.33,\ \rho^S = 1.34 Mg/m^3,\ \lambda^S = 5.5833 MN/m^2,\ \omega^* = 10/s,\ k^F = 0.01 m/s,$$
$$\mu^S = 8.3750 N/m^2,\ \gamma^{FR} = 10.00 KN/m^3 \text{ and } \rho^F = 0.33 mg/m^3 \qquad (6.1)$$

In medium M_2

$$\bar{\eta}^S = 0.6,\ \bar{\eta}^F = 0.4,\ \bar{\rho}^S = 2.0 Mg/m^3,\ \bar{\lambda}^S = 4.2368 MN/m^2,\ \omega^* = 10/s$$
$$\bar{k}^F = 0.02 m/s,\ \bar{\mu}^S = 3.3272 N/m^2,\ \bar{\gamma}^{FR} = 9.00 KN/m^3,\ \rho^F = 0.33 mg/m^3,\ k_n = 0.5,\ k_t = 0.25 \qquad (6.2)$$

For this model to represent different reflected and refracted waves amplitude ratios graphically a MATLAB program is constructed. The amplitude ratios of waves are determined for incidence angle which varies from $\theta_0 = 0^0$ to $\theta_0 = 90^0$ $|Z_i|(i = 1,2,3,4)$. The magnitudes of amplitude ratios corresponding to reflected P, reflected SV-wave, transmitted P, and transmitted SV-wave respectively. The variations in $|Z_i|$ with emergence angle θ_0 of P or SV-wave have been revealed in figures (1 to 8) and figures (9 to 40) for perfect and imperfect contact of the media at interface $z=0$ respectively.

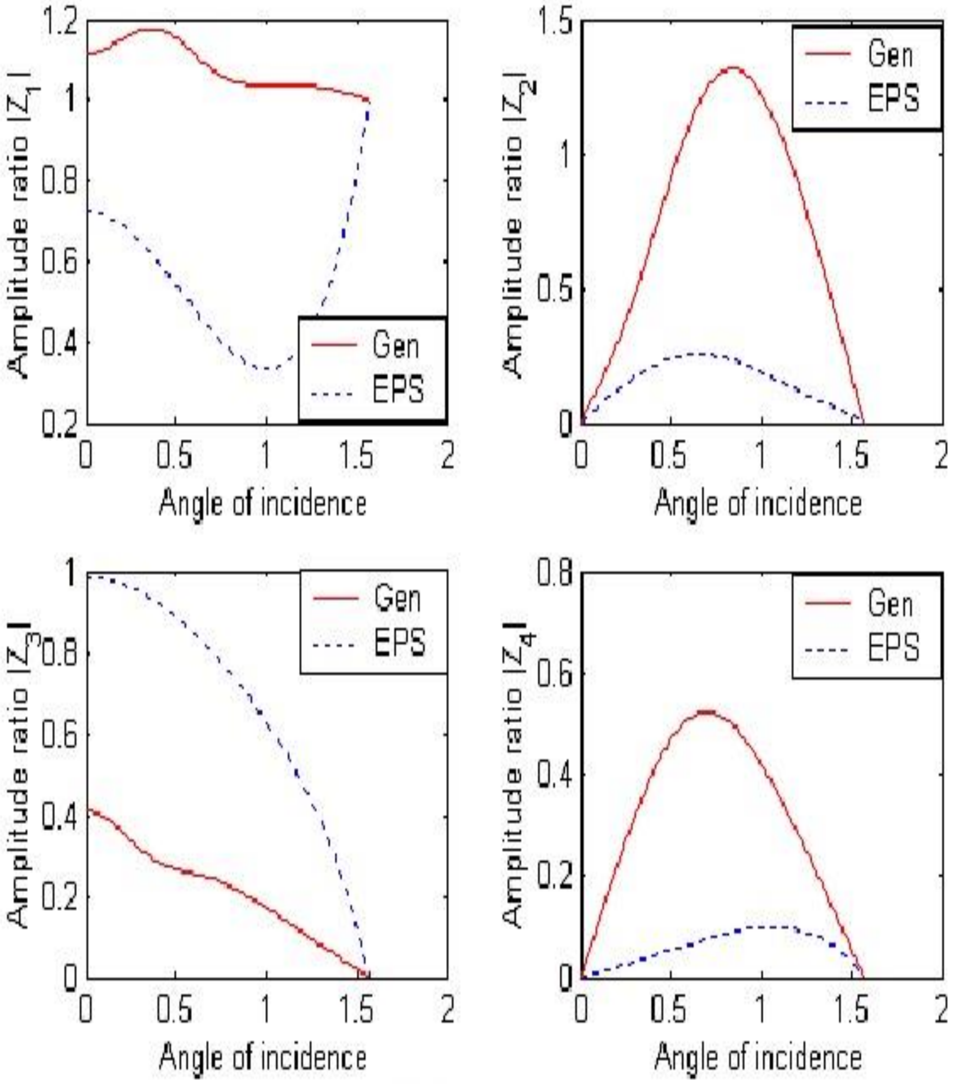

Figures (2) to (.4): Variation in amplitude ratios $|Z_i|$ (i = 1, 2, 3, 4) with respect to incidence angle of P-wave

The solid curve indicated by 'Gen' represents the case when media welded in contact. 'TFS' describe the particular case of transverse force stiffness interface and 'NFS' represent the case of normal force stiffness interface. Dotted lines' EPS' indicated when media M_1 & M_2, reduces to empty porous solid. 'Welded'/'Imperfect' represents the particular case when interface between the mediums is welded/imperfect in contact respectively. Figures (1) to (4), (5) to (20) and (5) to (8), (21) to (40) corresponding to P-waves and SV-waves are incident respectively.

The variation in amplitude ratios $|Z_i|\,(i=1,2,3,4)$ w.r.t. emergence angles $0^0 \le \theta_0 \le 90^0$, to study the effect of porosity on amplitude ratios when P-wave strikes at the interface have depicted in the figures (1) to (4). Effect of fluid is clearly visible on the modulus of amplitude ratios of reflected and refracted waves.

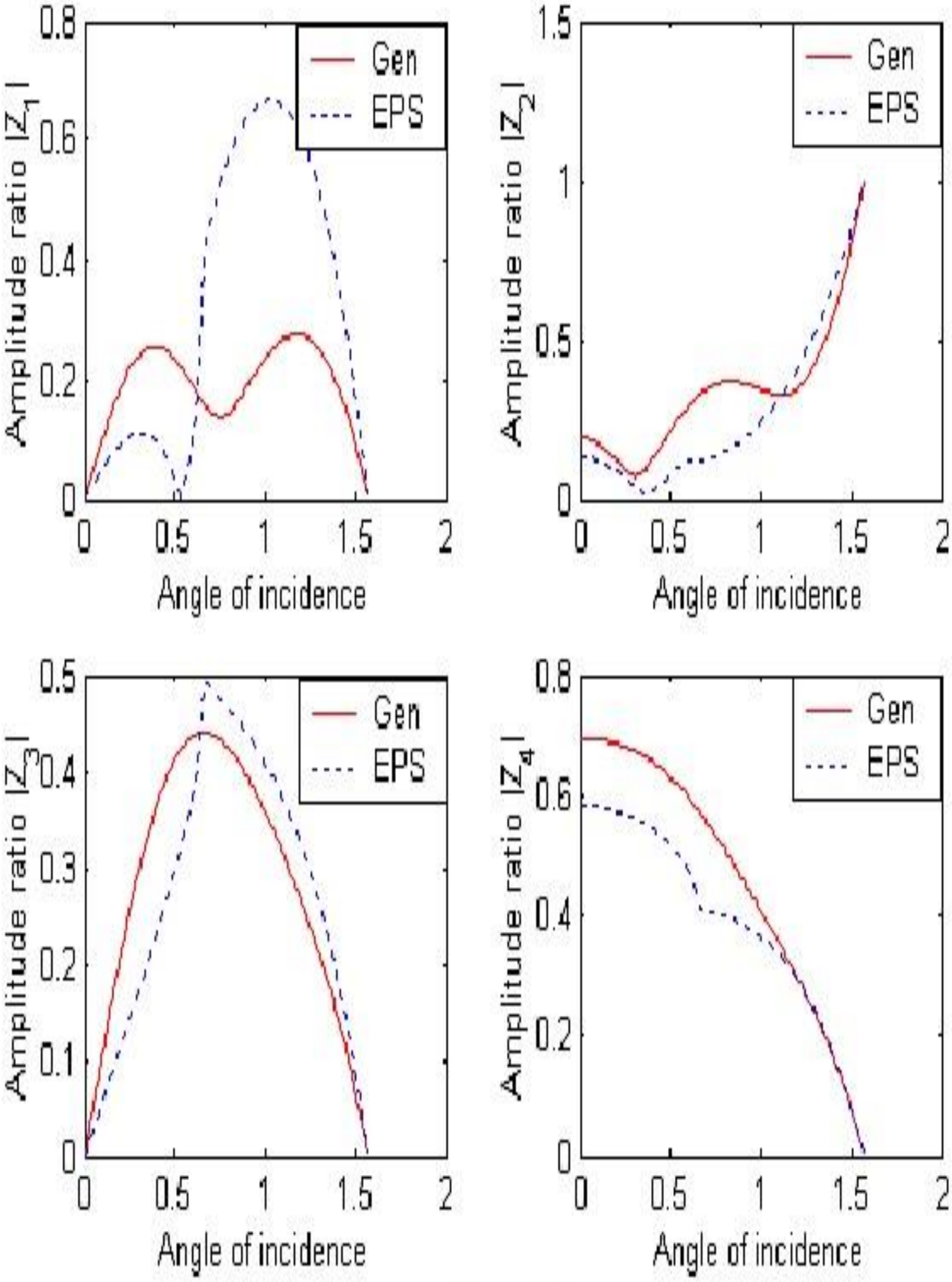

Figures (.5) to (.8): Variation in amplitude ratios $|Z_i|$ $(i = 1, 2, 3, 4)$ with respect to emergence angle of SV-wave

Now, from figures (5) to (8) the effect of porosity has drawn in the case when SV-wave strikes at the boundary of the perfect interface between the mediums. In this case, also, a significant part for the saturated porous medium is the effect of pores filled with fluid. To investigate the effect of nature of the emergent wave, compare the figures (2) to (4) with the figures (5) to (8) simultaneously. It established that the effect of the incident wave is computable on the modulus of the amplitude ratio.

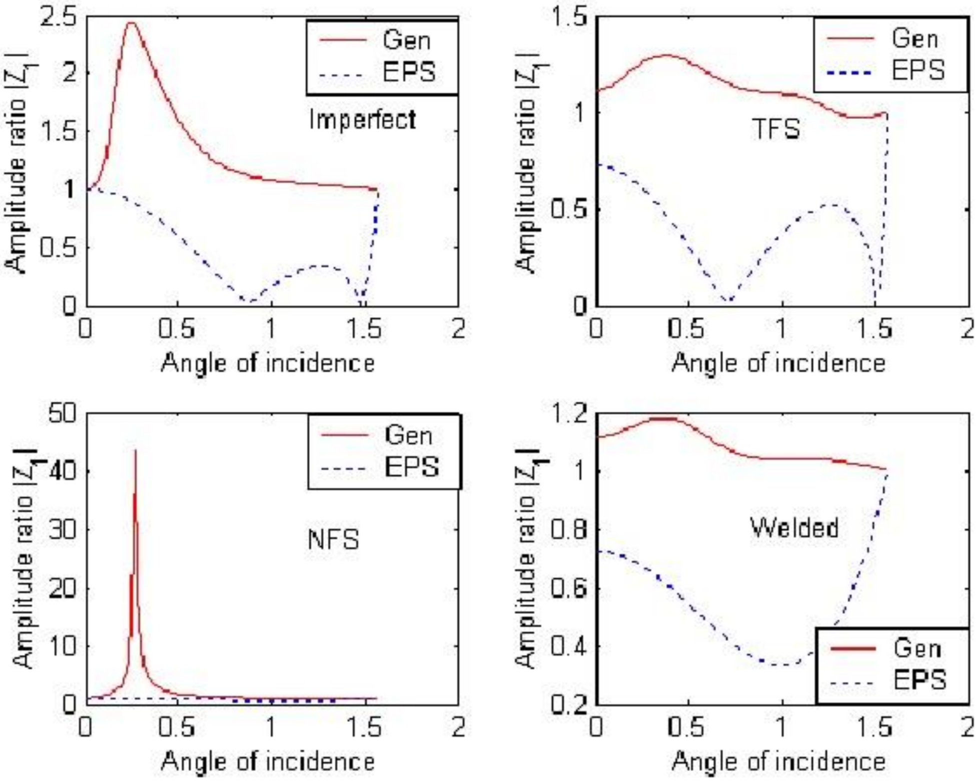

Figures (9) to (12): Variation in amplitude ratios $|Z_1|$ with respect to emergence angle of emergent P-wave

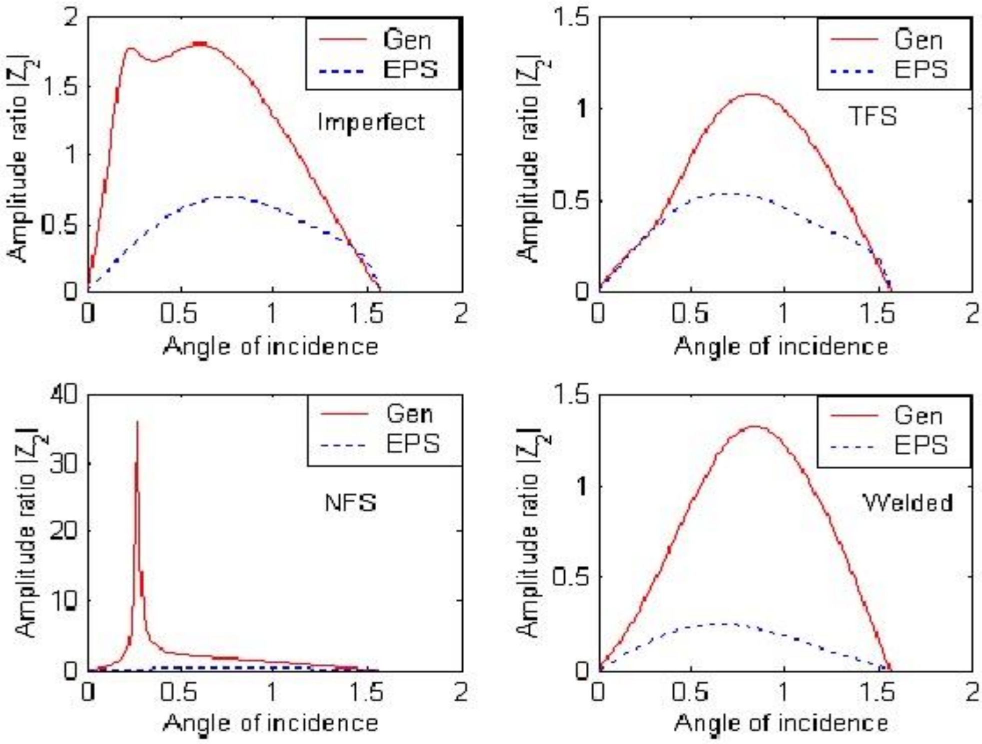

Figures (13) to (16): Variation in amplitude ratios $|Z_2|$ with respect to emergence angle of emergent P-wave

The effect of the boundary between the mediums on the modulus of amplitude ratio $|z_1|$ investigated from figures (9) to (12), which conclude that the consequences of the interface are considerable on the modulus of amplitude ratio. In addition, the value of amplitude ratio in Gen case is large than value of the ratio in EPS case and the porosity as well as boundary interface plays a momentous role on modulus of amplitude ratios.

Similarly, the effects of boundary considered and conclude in figures (13) to (16), which shows the effect of bonding parameter as well as effect of porosity of the medium on the modulus of amplitude ratios $|z_2|$.

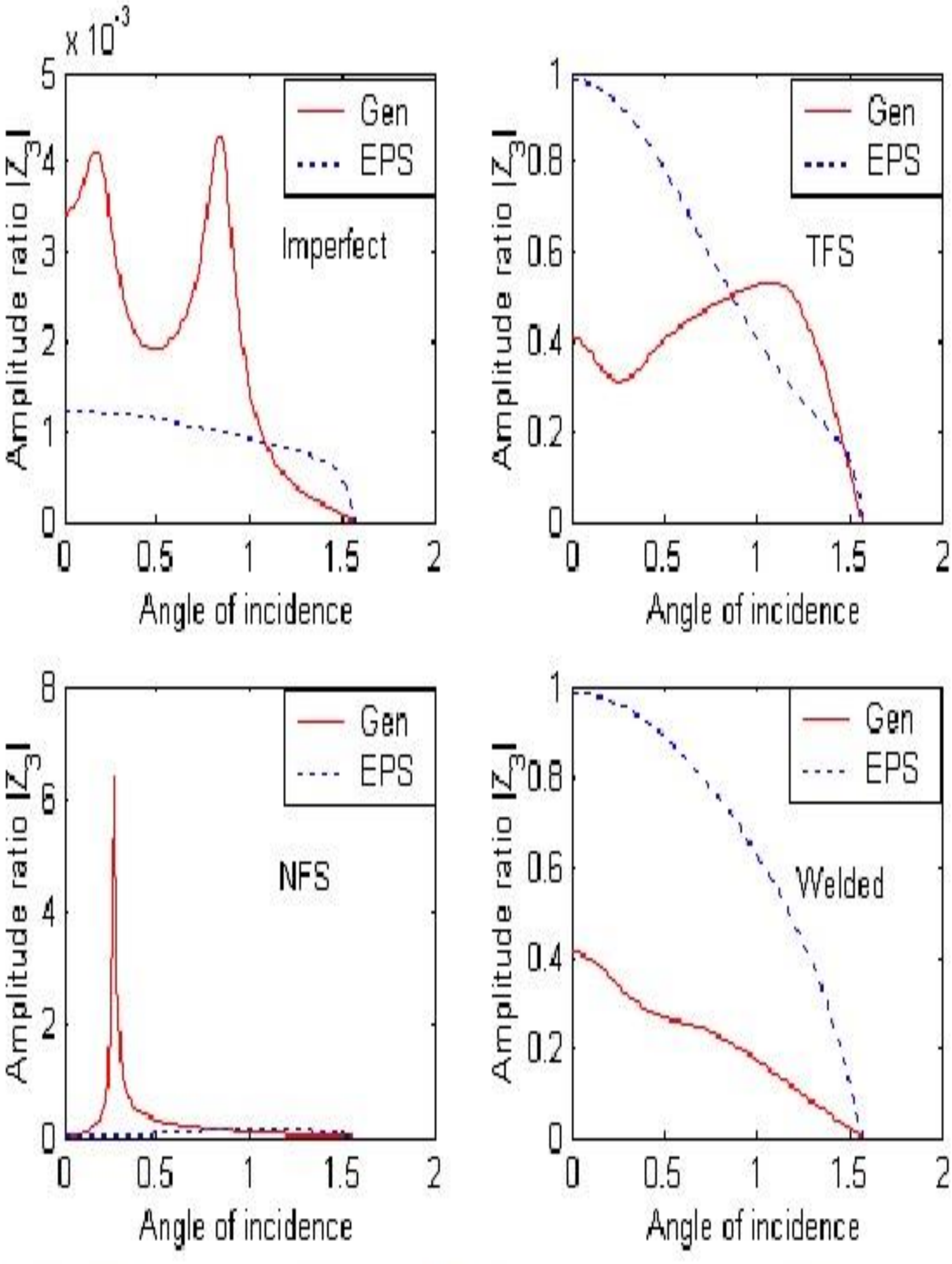

Figures (17) to (20): Variation in amplitude ratios $|Z_3|$ with respect to emergence angle of emergent P-wave

In continuous observations of behavior of amplitude ratios of $|z_3|$ from the figures (17) to (20) that depends upon the effect of porosity, boundary interface, fluid filled in the porous media, and effect of bonding parameter has significant effect on the amplitude ratios.

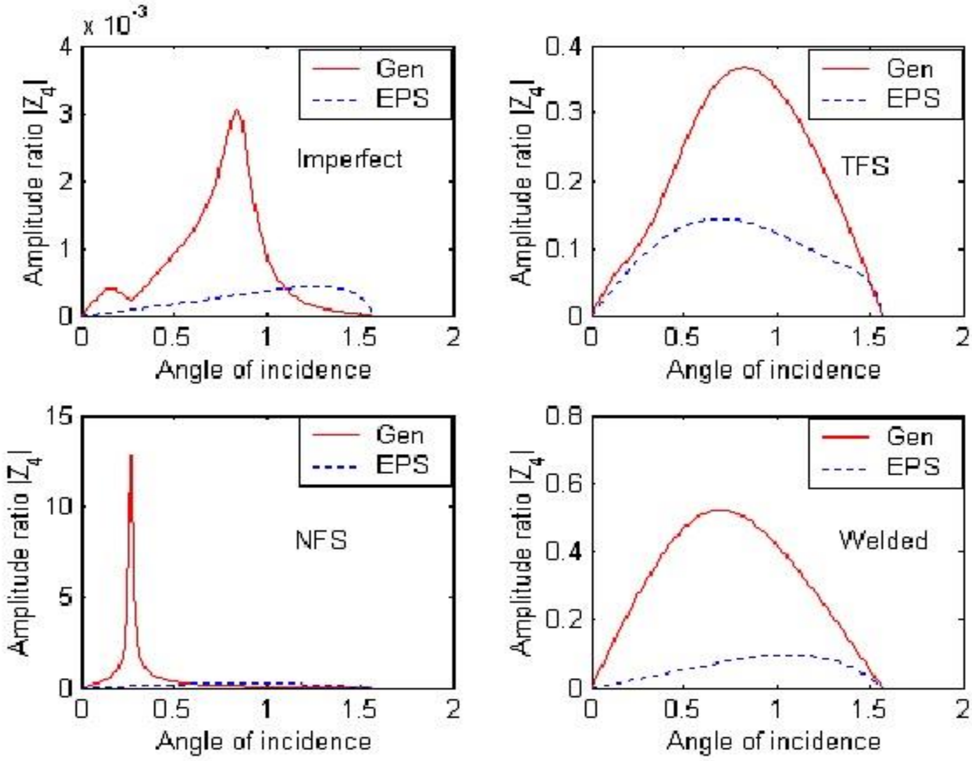

Figures (21) to (24): Variation in amplitude ratios $|Z_4|$ with respect to emergence angle of emergent P-wave

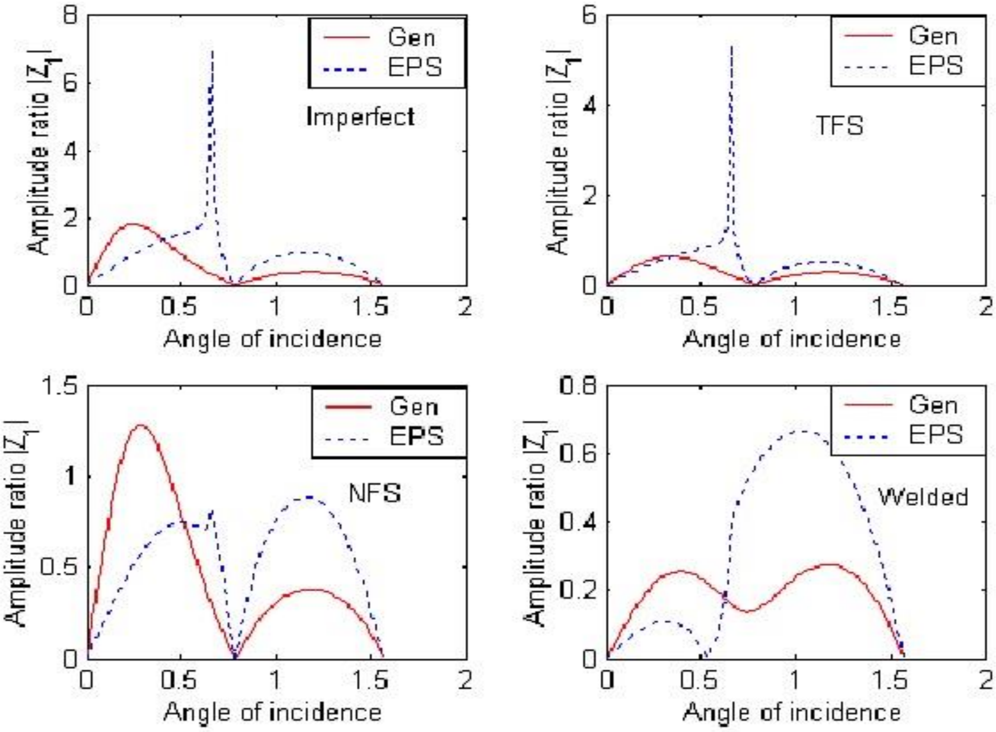

Figures (25) to (28): Variation in amplitude ratios $|Z_1|$ with respect to emergence angle of emergent SV-wave

Figures (21)-(24) and (25)-(28) concluded that the effect of bonding parameter and fluid filled in the porous media is considered as a momentous on the modulus of amplitude

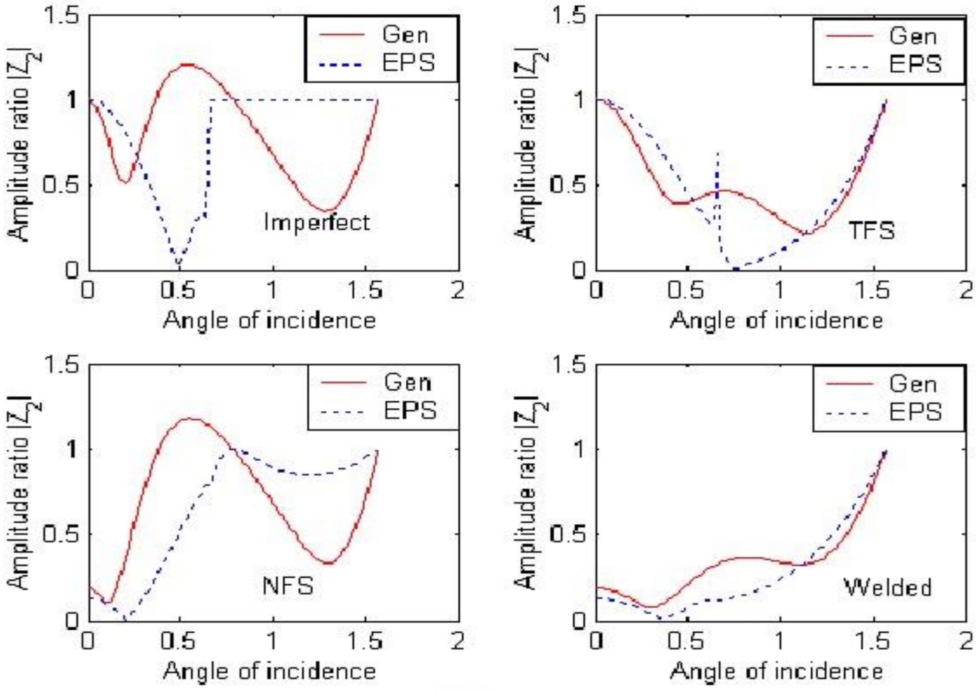

Figures (29) to (32): Variation in amplitude ratios $|Z_2|$ with respect to emergence angle of emergent SV-wave

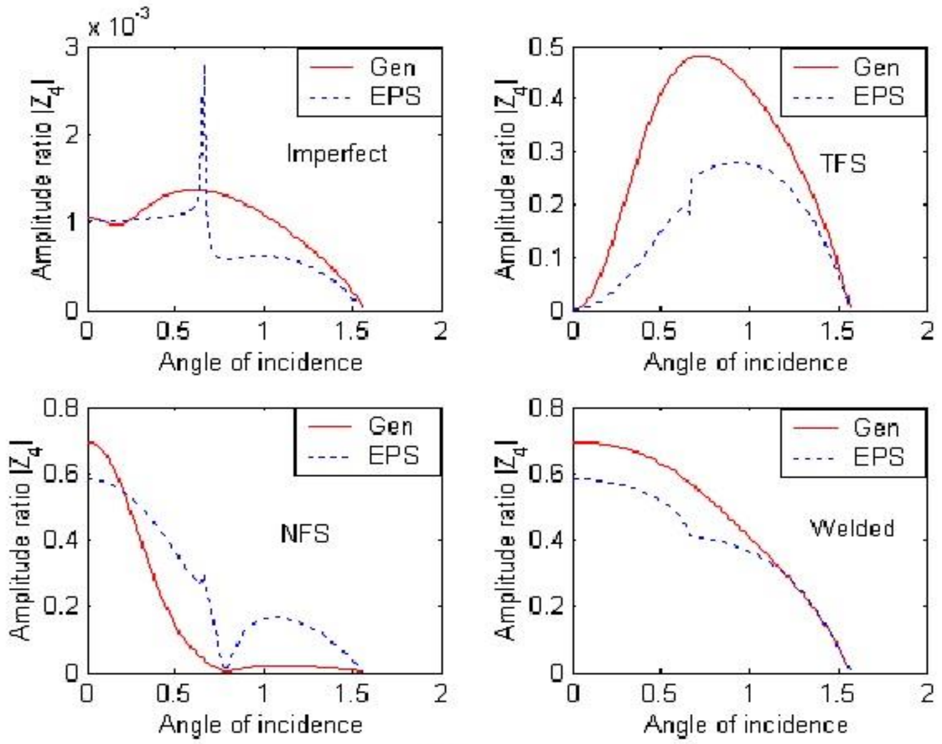

Figures (37) to (40):: Variation in amplitude ratios $|Z_4|$ with respect to emergence angle of emergent SV-wave

ratios $|Z_4|$ and $|Z_1|$ respectively. It can be stated that the effect of emergent wave (i.e. either P-wave is incident or SV-wave is incident at the interface) is noteworthy on the ratios. Characteristics of amplitude ratios $|Z_2|$, $|Z_3|$, and $|Z_4|$ in case of fluid filled in porous media can observed from the figures (29)-(32), (33)-(36), and (37)-(40) respectively.

From these figures, It is found that the effect of bonding parameter, fluid filled in the porous media are significant on the modulus of amplitude ratio $|Z_2|$, $|Z_3|$, and $|Z_4|$ respectively.

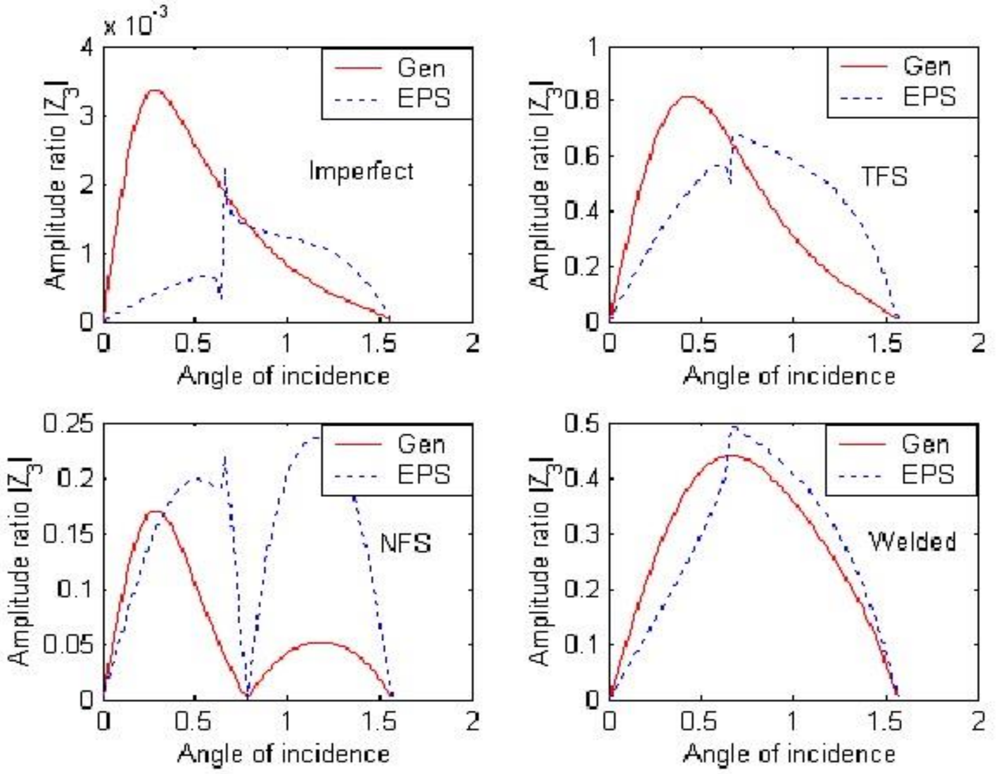

Figures (33) to (36): Variation in amplitude ratios $|Z_3|$ with respect to emergence angle of emergent SV-wave

Conclusion

The stresses, displacements and pore pressures of both media are obtained with help of potential functions. The amplitudes ratios of different reflected and refracted waves have been observed graphically with help of physical parameters and found that amplitude ratios of different reflected and transmitted waves depend on the incidence angle of emergent wave. Hence, we conclude that the amplitude ratios depend on emergence angle of emergent wave, material properties of medium, on incident wave, porosity of fluid drenched incompressible porous medium and stiffness of imperfect boundary.

7 **Highlight** The characteristic of amplitude ratios of various reflected and refracted wave has been analyzed which depend upon the emergence of angle of emergent waves, material properties of media, porosity of fluid saturated medium, and stiffness of the perfect/imperfect boundary.

8 **Conflict Statement** On behalf of all authors, the corresponding author states that there is no conflict of interest.

References

[1] R. M. Bowen, "Incompressible porous media models by use of the theory of mixtures," *Int. J. Eng. Sci.*, vol. 18, no. 9, pp. 1129–1148, 1980, doi: 10.1016/0020-7225(80)90114-7.

[2] S. Hajra and A. Mukhopadhyay., "Reflection and refraction of seismic waves incident obliquely at the boundary of a liquid-saturated porous solid.," *Bull. Seismol. Soc. Am.*, vol. 72, no. 5, pp. 1509–1533, 1982.

[3] R. de Boer and W. Ehlers, "The development of the concept of effective stresses," *Acta Mech.*, vol. 83, no. 1–2, pp. 77–92, 1990, doi: 10.1007/BF01174734.

[4] R. de Boer, W. Ehlers, and Z. Liu, "One-dimensional transient wave propagation in fluid-saturated incompressible porous media," *Arch. Appl. Mech.*, vol. 63, no. 1, pp. 59–72, 1993, doi: 10.1007/BF00787910.

[5] R. Kumar and M. L. Gogna, "Propagation of waves in a micropolar elastic layer with stretch immersed in an infinite liquid," *Proc. Indian Acad. Sci. - Math. Sci.*, vol. 98, no. 1, pp. 89–99, 1988, doi: 10.1007/BF02880975.

[6] R. Kumar and B. S. Hundal, "Symmetric wave propagation in a fluid-saturated incompressible porous medium," *J. Sound Vib.*, vol. 288, no. 1–2, pp. 361–373, 2005, doi: 10.1016/j.jsv.2004.08.046.

[7] R. Kumar and M. Barak, “Wave propagation in liquid-saturated porous solid with micropolar elastic skelton at boundary surface,” *Appl. Math. Mech. (English Ed.*, vol. 28, no. 3, pp. 337–349, 2007, doi: 10.1007/s10483-007-0307-z.

[8] R. W. Ogden and B. Singh, “Propagation of waves in an incompressible transversely isotropic elastic solid with initial stress: Biot revisited,” *J. Mech. Mater. Struct.*, vol. 6, no. 1–4, pp. 453–477, 2011, doi: 10.2140/jomms.2011.6.453.

[9] J. E. Santos and G. B. Savioli, “A parametric analysis of waves propagating in a porous solid saturated by a three-phase fluid,” *J. Acoust. Soc. Am.*, vol. 138, no. 5, pp. 3033–3042, 2015, doi: 10.1121/1.4934630.

[10] M. S. Barak and V. Kaliraman, “Propagation of Elastic Waves at Micropolar Viscoelastic Solid/Fluid-Saturated Incompressible Porous Solid Interface,” *Int. J. Comput. Methods*, vol. 15, no. 8, pp. 1–19, 2018, doi: 10.1142/S0219876218500767.

[11] M. Kumar, M. Kumari, and M. S. Barak, “Reflection of plane seismic waves at the surface of double-porosity dual-permeability materials,” *Pet. Sci.*, vol. 15, no. 3, pp. 521–537, 2018, doi: 10.1007/s12182-018-0245-y.

[12] M. Kumar, M. S. Barak, and M. Kumari, “Reflection and refraction of plane waves at the boundary of an elastic solid and double-porosity dual-permeability materials,” *Pet. Sci.*, vol. 16, no. 2, pp. 298–317, 2019, doi: 10.1007/s12182-018-0289-z.

[13] M. S. Barak and V. Kaliraman, “Reflection and transmission of elastic waves from an imperfect boundary between micropolar elastic solid half space and fluid saturated porous solid half space,” *Mech. Adv. Mater. Struct.*, vol. 26, no. 14, pp. 1226–1233, 2019, doi: 10.1080/15376494.2018.1432795.

[14] M. S. Barak, M. Kumar, M. Kumari, and A. Singh, “Inhomogeneous wave propagation in partially saturated soils,” *Wave Motion*, vol. 93, 2020, doi: 10.1016/j.wavemoti.2019.102470.

[15] M. Kumar, A. Singh, M. Kumari, and M. S. Barak, “Reflection and refraction of elastic waves at the interface of an elastic solid and partially saturated soils,” *Acta Mech.*, vol. 64, no. 3, pp. 293–317, 2020, doi: 10.1007/s00707-020-02819-z.

[16] H. Ghasemzadeh and A. A. Abounouri, “Compressional and shear wave intrinsic attenuation and velocity in partially saturated soils,” *Soil Dyn. Earthq. Eng.*, vol. 51, pp. 1–8, 2013, doi: 10.1016/j.soildyn.2013.03.011.

[17] O. Ifayefunmi, F. M. Mahidan & S. H. Wang, " Buckling of Cones with Imperfect Length Subjected to Axial Compression ", International Journal of Mechanical and Production Engineering Research and Development (IJMPERD), Vol. 9, Issue 4,pp, 219-228

[18] Amaresh Kumar D, Atmanand Anikivi & Shridhar Deshpande, “FEA Analysis and Optimization of Two-Wheeler Bike Mono Suspension System”, International Journal of Mechanical and Production Engineering Research and Development (IJMPERD), Vol. 9, Issue 2, pp, 111-122

[19] Radhika Rani L & Chandralingam S, "Acoustic Analysis of Cry Signal To Differentiate Healthy and Congenital Heart Disorder in Infants", International Journal of Electronics and Communication Engineering (IJECE), Vol. 5, Issue 6, pp; 21-28

[20] Rashmi R. Keshvani & Maulik S. Joshi, " A Study about Soil Temperature Variation at Distinct Sub-Surfaces ", IMPACT: International Journal of Research in Engineering & Technology, Vol. 6, Issue 3, pp, 29-32

[21] Adeyemo, I. A, Ojo, J. A. & Adegbola, O. A, "Performance Evaluation of Three Evolutionary Algorithms for 27 Selective Harmonic Elimination in Voltage Source Multilevel Inverter", BEST: International Journal of Management, Information Technology and Engineering (BEST: IJMITE), Vol. 3, Issue 10, pp, 25-42

[22] Hossein Rasekh, Mahmood Ghasemi & Mohsen Sadeghi, " Employing Positive Feedback Technique to Improve Simultaneously UGBW and Gain for Op-Amps ", BEST: International Journal of Management, Information Technology and Engineering (BEST: IJMITE), Vol. 1, Issue 3, pp, 1-4